

# Medical image segmentation using a tree model

V. Grau, M. Alcañiz, C. Monserrat, M.C. Juan, J.A. Gil

MedICLab, Universidad Politécnica de Valencia, Camino de Vera, 46022 Valencia, Spain  
vgrauc@degi.upv.es

**Abstract-** A model-driven, multiscale medical image segmentation system is presented. A tree representation is calculated for the image, using a modification of the immersion algorithm used for watersheds calculation. Segmentation is carried out by a matching process between the obtained tree and a tree model, which embeds the prior knowledge about the images. Tree matching is done in a multilevel way, processing different tree levels sequentially. For each level, an optimization process is performed, in which an error function, obtained from differences between the model and the segmented tree, is minimized. 13 parameters, concerning gray level, shape, position and connectivity, are used to characterize the objects. The model is obtained from a set of training images, assigning manual labels to tree nodes with a user interface designed especially for this purpose. Three-dimensional, multicomponent images can be processed by adapting gradient and parameter calculation. The system has been tested for intracranial cavity segmentation in magnetic resonance images, giving accurate results.

**Keywords-** Medical image analysis, model-driven segmentation, multiscale, watersheds

## I. INTRODUCTION

Medical image segmentation remains an open problem in many different applications. Many researchers have given specific, ad hoc solutions for certain problems. General segmentation schemes, however, are far from being accurate for a majority of cases [1].

It is unlikely that a correct automatic segmentation could be obtained without relying on prior knowledge about the images. For this purpose, the utilization of anatomical models is a good way to represent this knowledge [2], [3].

In the search for an adequate model of image structure, multiscale approaches have received special attention [4], [5]. Compact descriptions can be achieved by using singular points of the image. Several research studies have been carried out to study the behaviour of these points under the application of filters. Local extrema of the image can be used as the special points for such study: combined with mathematical morphology filters, it is possible to obtain a multiscale description [6], providing interesting advantages: local extrema suffer no displacement under the application of dilation-erosion filters; furthermore, a complete segmentation of the image, at different scales, is easily obtained by watersheds calculation [7].

A tree description is especially adequate to represent segmentations at different scales. These trees can be obtained efficiently by using a modification of the immersion algorithm for watershed calculation [8]. Each node of the tree corresponds to a minimum of the gradient, while its height in the tree indicates the corresponding scale.

We have developed a system that obtains a complete segmentation of the image by calculating efficiently its tree representation, matching it then with a tree model, which contains the prior knowledge about the images. All the aspects of the process, including model calculation, are explained in the following section.

## II. METHODOLOGY

### A. Previous Steps

Watersheds are calculated on the gradient of the original image. For multicomponent three-dimensional images, the *vector gradient*, as defined in [9] is used. Calculation of the gradient components in the three axes is carried out using the Sobel operator.

The original images are filtered using an anisotropic three-dimensional filter [10] to reduce the effect of noise. After gradient calculation, a dual h-reconstruction [6] is applied to reduce the number of minima of the gradient image, which corresponds directly to the number of regions that result from the watersheds calculation.

### B. Tree Calculation

The immersion algorithm calculates efficiently the watersheds of the image. This technique uses an analogy with the gradual immersion of a topological surface (the image, in which high gray levels are interpreted as high elevations, and vice versa), into water. We have implemented a modification of this technique, in which the catchment basins merge during the process to produce higher-level regions, as shown in fig. 1 for a one-dimensional signal (two- or three- dimensional signals are processed in the same way). In this case, the normal immersion process would have produced four regions, labelled as 1-4 in fig. 1. Our modification maintains these regions, while adding high-level nodes 5 and 6. To avoid an excessive number of nodes, new ones are created only if necessary: in figure 1, when regions 5 and 6 merge, a link is created instead of a new node. The direction of this link (that is, which one of the two nodes becomes the father) depends on the *extinction value* of the corresponding minima, which in fig. 1 corresponds simply to the size of the region at the merging time: region 5 is larger in this case. Other extinction values, such as the dynamics (depth of the minima) can also be applied without changing the tree building algorithm.

## Report Documentation Page

<b>Report Date</b> 25OCT2001	<b>Report Type</b> N/A	<b>Dates Covered (from... to)</b> -
<b>Title and Subtitle</b> Medical image segmentation using a tree model		<b>Contract Number</b>
		<b>Grant Number</b>
		<b>Program Element Number</b>
<b>Author(s)</b>		<b>Project Number</b>
		<b>Task Number</b>
		<b>Work Unit Number</b>
<b>Performing Organization Name(s) and Address(es)</b> MedICLab, Universidad Politécnica de Valencia, Camino de Vera, 46022 Valencia, Spain		<b>Performing Organization Report Number</b>
<b>Sponsoring/Monitoring Agency Name(s) and Address(es)</b> US Army Research Development & Standardization Group (UK) PSC 802 Box 15 FPO AE 09499-1500		<b>Sponsor/Monitor's Acronym(s)</b>
		<b>Sponsor/Monitor's Report Number(s)</b>
<b>Distribution/Availability Statement</b> Approved for public release, distribution unlimited		
<b>Supplementary Notes</b> Papers from the 23rd Annual International Conference of the IEEE Engineering in Medicine and Biology Society, October 25-28, 2001, held in Istanbul, Turkey. See also ADM001351 for entire conference on CD-ROM.		
<b>Abstract</b>		
<b>Subject Terms</b>		
<b>Report Classification</b> unclassified	<b>Classification of this page</b> unclassified	
<b>Classification of Abstract</b> unclassified	<b>Limitation of Abstract</b> UU	
<b>Number of Pages</b> 4		

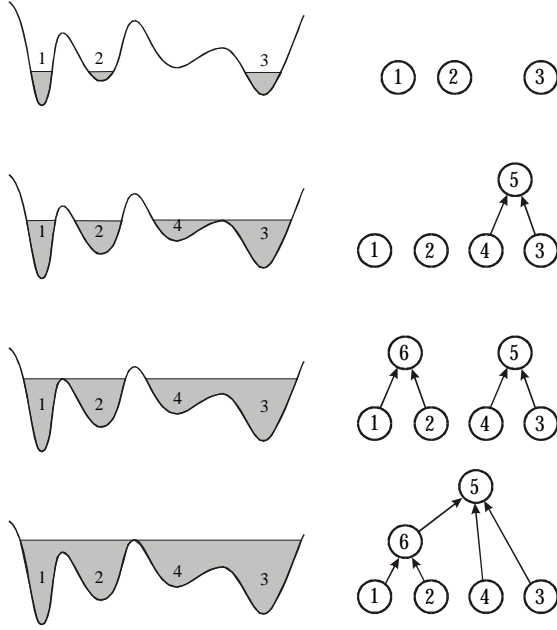


Figure 1. Construction of the tree during the immersion process

Complete segmentations can be obtained at different scales, by taking the nodes at the appropriate level and considering the regions associated with each one of them. In fig. 1, the coarsest scale is represented only by node 5, which covers all the domain, while the finest one corresponds to the output of the unmodified immersion procedure, that is, nodes 1, 2, 3, 4.

### C. Model Obtaining

Image segmentation is achieved by transformation of the tree obtained by the modified immersion algorithm into a tree model, which embeds the prior knowledge about anatomical objects. This model is obtained from manual segmentation of a set of training images.

Manual segmentation is carried out in the following way: a tree, corresponding to the first training image is constructed, as described. Manual labelling of the obtained nodes is then performed using an interactive user interface. Labels can be assigned at any scale level of the tree, thus minimizing segmentation time. After the first image has been accurately segmented, a pruning process is applied to obtain a simplified tree, in which each label corresponds to a single tree node. The tree topology obtained in this first segmentation is manually validated by the user, and can be modified to eliminate small nodes, which may appear at undesired locations of the tree. This topology is preserved throughout the rest of the training process.

Once topology has been determined, the following parameters are obtained for each node of the model tree:

- Gray level parameters: Mean value, standard deviation and maximum/minimum values. For multicomponent images, all those parameters are calculated for each image component.
- Shape parameters: Area, perimeter, compactness, central second-order moments  $\mu_{20}$  and  $\mu_{02}$ , eccentricity and orientation of the major axis are used. In case we work with three-dimensional images, volume and external area are used instead of area and perimeter, second-order moments used are  $\mu_{200}$ ,  $\mu_{020}$  and  $\mu_{002}$ , and orientations of the main and the second axes are used.
- Node centroid

Parameters are calculated for all the training images, and their mean and maximum deviation are stored. The use of these values is explained further in the next section.

### D. Tree Matching

To segment a new image, a matching process between its corresponding tree, calculated as described in section II.B, and the model for this type of images, is carried out. The usual situation is the following: the tree obtained from the new image, which contains hundreds of nodes, must be transformed into a much simpler model. So we can assume that the transformation of the new tree into the model is always a tree simplification.

This simplification problem can be solved by performing a *classification*: the nodes of the tree model can be seen as classes, which must be assigned to the nodes of the new tree. Classification is carried out hierarchically, starting at the coarsest level of both trees and descending step by step.

At each level, classification is carried out by an optimisation process, in which an error function is minimized. This error function quantifies the difference, at the current scale, between the tree model and the classification, and is defined as follows:

$$Err = \sum_{i=1}^K \sum_{j=1}^F \Phi(|f_{ij}(\text{new}) - f_{ij}(\text{model})|) \quad (1)$$

where K is the number of classes (nodes of the model at the current scale), F is the total number of parameters used (listed in section II.B),  $f_{ij}$  represents the value of parameter j in class i, and  $\Phi$  is the weighting function that is shown in fig. 2. Two parameters must be determined:  $\Delta_{ij,lim}$ , which corresponds to the maximum “zero error” value, and the slope of the function,  $w_{ij}$ . They are determined from the manual segmentations of the training images, as follows:

- $f_{ij}(\text{model})$  is the mean value of parameter j in class i of the images in the training set;

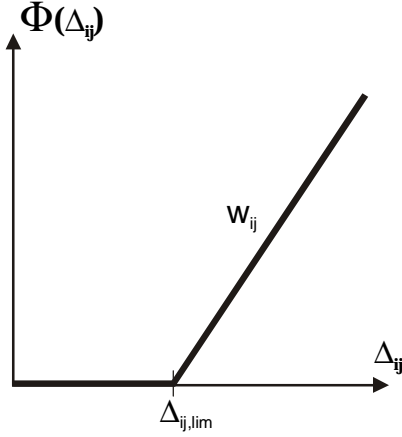


Figure 2. Weighting function used in error calculation

- $\Delta_{ij,lim}$  receives the value of the highest difference from the mean value of parameter  $j$  in class  $i$ . In this way, it is assured that all the manual segmentations given to the training images have zero error.
- $w_{ij}$  can be adjusted to assign different weights to different parameters or classes. In our case,  $w_{ij}$  is assigned the inverse of  $\Delta_{ij,lim}$ , so that differences produce a stronger penalization for parameters with a smaller spread.

An important condition that should be achieved is *connectivity*, i.e., that each node in the model tree should correspond to a single connected component of the labelled image. So we define the connectivity parameter as follows:

$$Con(i) = \frac{A_{\max \text{ comp}}(i)}{A(i)} \quad (2)$$

where  $A_{\max \text{ comp}}(i)$  is the area of the maximum connected component of node  $i$ , and  $A(i)$  the total area of this node. For three-dimensional images, area is substituted by volume in (2).

As we have mentioned, connectivity should always reach a value of 1 at the end of the optimisation process. A high weight of the connectivity does not assure that this condition is always reached and, moreover, causes local minima of the error function to appear. To prevent these complications, we apply initially a zero weight to the connectivity, until the process converges to a minimum. This weight is then progressively incremented until total connectivity is achieved.

The optimization process, at each level, consists of a series of movements in the space of possible classifications. Two types of movements are allowed:

- Label change: assignation of a different label to a node.
- Node splitting: one of the nodes is partitioned into different classes, by taking all its direct descendants and assigning them different labels.

Initial classification is important, as it can affect the process in two ways: avoiding local minima of the error

function and reducing the number of movements necessary. Prior knowledge about the specific segmentation problem could be much useful to determine the initialization state. Anyway, to keep the segmentation system applicable to any type of medical image, we take as initial state the best one of a number of random solutions.

The optimization technique used is the steepest descent algorithm: at each state, all its *neighbors* (that is, all the steps that can be reached with a single movement) are tested, and the one with the smallest error is taken. In case none of the neighbors has an error smaller than the current value, a minimum has been reached, so the optimization process stops.

In order to prevent the system getting stuck in a local minimum, several initial values, taken at random locations, are tried. The final solution is the best one obtained from these different initial locations.

### III. RESULTS

To demonstrate the applicability of the system to medical images, it has been used to segment the intracranial cavity (ICC) from magnetic resonance images of patients with multiple sclerosis. A simple tree was generated, in which the head is first extracted, followed by a classification in three classes: skin, bone and ICC. The tree model is shown in fig. 3.

The system was trained using 10 images of different patients. One central slice, at approximately the same location, was taken from each study. The trained tree was then used to segment a different set of images. Some results are shown in fig. 4, where head and ICC contours are superimposed on the original images: as can be seen, results are qualitatively correct. Cases such as the lower left of fig. 4, where cortical bone is thin, are especially challenging to conventional, gray-based only techniques, as it is difficult to separate ICC from bone. In our system, the introduction of shape parameters and the minimization of a global function allow to obtain correct results even in these cases. Calculation time needed to process the images in fig. 4 was between 1 and 3 minutes in a PC Pentium III.

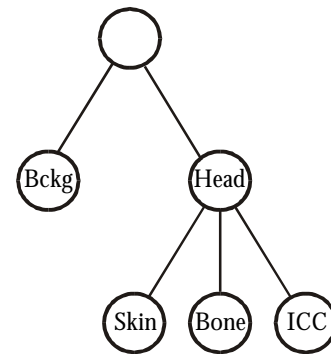


Figure 3. Tree model used for segmentation of intracranial cavity

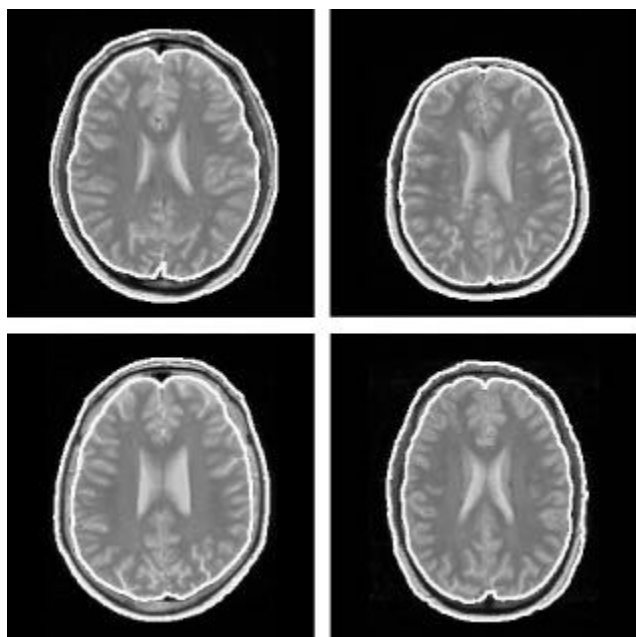


Figure 4. Results for head and ICC contours of different patients

#### IV. DISCUSSION

Many different applications of medical images require segmentation of the anatomical structures. Specific systems have been developed for special applications. However, if segmentation of a different object is needed, or even if the acquisition parameters vary, application-specific systems must be deeply redesigned for the new application.

We have developed a system that separates the segmentation process from the a priori knowledge of the images (the model), so that, if we have to segment a different type of image, only this model must be recalculated. Furthermore, we have designed an efficient way to determine the models, starting from the original tree. This model calculation interface can also be used independently as a semiautomatic segmentation system.

The system can work on three-dimensional, multicomponent images. Processing time, however, may be a problem if very big data volumes are used. Alternatives for parallel calculation of the data are being studied.

The system presented has demonstrated its performance in segmentation of the intracranial cavity from MR images. A detailed quantitative evaluation is being carried out at the moment. Different applications, such as liver segmentation from CT-MR images, will also be tested.

#### IV. CONCLUSION

A new, general purpose medical image segmentation system has been presented. The use of a tree model makes the system easily applicable to different anatomical locations or modalities. The system works on 3-D, multicomponent images, thus taking profit of multimodal patient explorations. Initial results have demonstrated the applicability of the system to specific medical problems.

#### REFERENCES

- [1] J.S. Duncan and N. Ayache, "Medical image analysis: progress over two decades and the challenges ahead," *IEEE Trans. Pattern Analysis and Machine Intelligence*, vol. 22, no. 1, pp. 85-105, January 2000
- [2] M. Sonka, S.K. Tadikonda and S.M. Collins, "Knowledge-based interpretation of MR brain images," *IEEE Trans. Med. Imaging*, vol. 15, no. 4, pp. 443-452, August 1996
- [3] S.M. Pizer, D.S. Fritsch, P.A. Yushkevich, V.E. Johnson and E.L. Chaney, "Segmentation, registration, and measurement of shape variation via image object shape," *IEEE Trans. Med. Imaging*, vol. 18, no. 10, pp. 851-865 October 1999
- [4] A. Simmons, S.R. Arridge, P. S. Tofts and G.J. Barker, "Application of the extremum stack to neurological MRI," *IEEE Trans. Med. Imaging*, vol. 17, no. 3, pp 371-382, June 1998
- [5] Koster, A.S.E., Vincken, K.L., de Graaf, C.N., Zander, O.C., Viergever, M.A., "Heuristic linking models in multiscale image segmentation", *Computer Vision and Image Understanding*, v. 65, n. 3, pp. 382-402, 1997
- [6] Serra, J. *Image Analysis and Mathematical Morphology*. Academic Press, London, 1988.
- [7] J. Gauch, "Image segmentation and analysis via multiscale gradient watershed hierarchies," *IEEE Trans. Image Processing*, vol. 8, no. 1, pp. 69-79, January 1999
- [8] L. Vincent and P. Soille, "Watersheds in digital spaces: an efficient algorithm based on immersion simulations," *IEEE Trans. Pattern Analysis and Machine Intelligence*, vol.13, no.6, pp. 583-598, June 1991
- [9] H.-C. Lee and D.R. Cok, D.R., "Detecting boundaries in a vector field," *IEEE Trans. Signal Processing*, vol. 39, no. 5, pp. 1181-1194, May 1991
- [10] G. Gerig, O. Kübler, R. Kikinis and F.A. Jolesz, "Nonlinear anisotropic filtering of MRI data," *IEEE Trans. Medical Imaging*, vol. 11, no. 2, pp. 221-232, June 1992